

Chemical Shifts in ESCA and NMR: The Case of Bridged Trichlorosilyl-Trimethylsilyl Molecules

Shin-ichi Nagaoka,*[1] Umpei Nagashima,[2] and Joji Ohshita[3]

[1]Department of Chemistry, Faculty of Science, Ehime University, 2-5 Bunkyo-cho, Matsuyama 790-8577

[2]Grid Technology Research Center, AIST Tsukuba Central 2, 1-1-1 Umezono, Tsukuba 305-8568

[3]Department of Applied Chemistry, Faculty of Engineering, Hiroshima University, 1-4-1 Kagamiyama, Higashi-Hiroshima 739-8527

Received July 19, 2005; E-mail: nagaoka@ehimegw.dpc.ehime-u.ac.jp

A detailed examination of the relationship between chemical shifts in ESCA (electron spectroscopy for chemical analysis) and NMR (nuclear magnetic resonance) is presented for two silicon sites of bridged trichlorosilyl-trimethylsilyl molecules [$Cl_3Si–C_nH_m–Si(CH_3)_3$ ($n = 0–5$ and $m = 0–10$)]. It is shown that the ESCA chemical shift of a silicon site mainly depends on the electronic environment within a mean radius of 1.168 Å of the nucleus and the NMR chemical shift depends on the electronic environment within a radius of more than 1.875 Å.

The distinctive term "chemical shift" to designate the position of a spectral signal is mainly used in two forms of spectroscopy, ESCA (electron spectroscopy for chemical analysis) and NMR (nuclear magnetic resonance),[1] which have proven to be very useful for studies of the electronic structures of molecules. The chemical shifts in both ESCA and NMR reflect the electronic environment around an atomic site.

The phenomenon that came to be called "chemical shift in NMR" was first observed in 1950,[2–4] and the term "chemical shift" soon appeared in a paper.[5] The actual magnetic field experienced by a nucleus in a molecule differs very slightly from the applied field owing to the magnetic field produced by the molecular electrons. Since the magnetic field thus produced depends strongly on the chemical environment around the nucleus, the NMR frequency of the nucleus also depends on it. A shift in the resonance due to a specific chemical environment is called a "chemical shift in NMR."

The first evidence of the chemical shift in ESCA was obtained in 1958.[6–8] In contrast to valence electrons, which are often delocalized over the entire molecule, core electrons are localized near the atom of origin. Although core electrons do not participate in chemical bonding, the energy of an atomic core-level in the molecule depends on the chemical environment around its atom. A shift in the core-level energy due to a specific chemical environment is called a "chemical shift in ESCA."

Why the term, chemical shift, used for NMR was also applied to ESCA is not noted in the literature.[7] Was it intentional or coincidental? Regardless, after the finding of these types of chemical shift, systematic collection of ESCA and NMR data began,[9,10] and these chemical shifts have provided very important information on the electronic environment associated with chemical interaction between an atomic site and its surrounding atoms (and/or groups of atoms).

Although the same term, chemical shift, is used in ESCA and NMR, a general correlation between the two types of chemical shift has not been found.[11,12] In our opinion, the reason for this is that the spatial range of the electronic environment affecting the chemical shift in ESCA is different from that in NMR. A chemical shift reflecting the electronic environment in a small space around an atomic site cannot be expected to show a linear relationship with another chemical shift reflecting the electronic environment in a large space around the atomic site.

To determine the spatial ranges of the electronic environments affecting these two chemical shifts, we attempted to study the ESCA and NMR chemical shifts of bridged trichlorosilyl-trimethylsilyl molecules [$Cl_3Si–C_nH_m–Si(CH_3)_3$ ($n = 0–5$ and $m = 0–10$)] (Fig. 1). Our reasons for using these molecules in this study are as follows. First, in these molecules, the chemical environment around the Si atom bonded to three Cl atoms (Si[Cl]) is very different from that around the other Si atom bonded to three CH_3 groups (Si[Me]), because a Cl atom and a CH_3 group are, respectively, electron-accepting and -donating.[13,14] Accordingly, the two Si sites have the potential to show different chemical shifts in ESCA and NMR. Second, a general spectroscopic standard such as tetramethylsilane (TMS in Fig. 1) in chemical shifts of ^{1}H NMR[1,10]

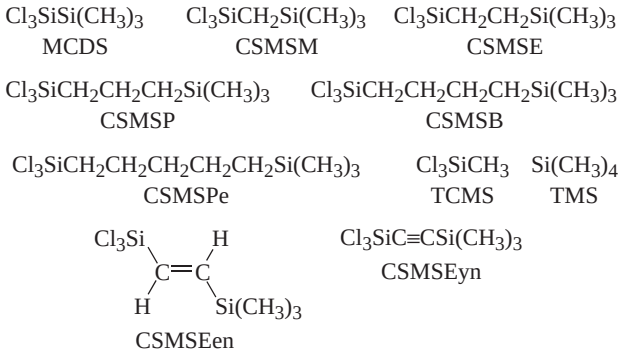

Fig. 1. Structures of molecules used in the present work.

Published on the web April 7, 2006; DOI: 10.1246/bcsj.79.537

is absent in ESCA. Thus, the bridged trichlorosilyl-trimethylsilyl molecules with the two Si sites are useful, because the difference between the two corresponding spectral positions can be taken as a shift in ESCA. Third, since the Cl_3Si– and –$Si(CH_3)_3$ groups are respectively electron-accepting and -donating,[13,14] it is interesting how the inter-site interaction affects the ESCA and NMR chemical shifts and how these chemical shifts depend on the length and bond order of the bridge (–C_nH_m–).

In the present study, we have obtained ESCA and NMR chemical shifts for the bridged trichlorosilyl-trimethylsilyl molecules by means of spectroscopic methods[1] and ab initio molecular-orbital calculations.[15] The ESCA chemical shifts in the binding energies of the Si:1s and 2p core electrons of these molecules have been studied, and the chemical shifts of ^{29}Si NMR have also been investigated. In this paper, the variations in ESCA and NMR chemical shifts according to the length and bond order of the bridge are discussed along with the relevant electronic structure. From these results, we will show the spatial ranges of the electronic environment affecting the chemical shifts in ESCA and NMR. The final goal of our study is to bridge the gap between the ESCA and NMR chemical shifts.

Experimental

Sample Preparation. Preparation of 1-(Trichlorosilyl)-4-(trimethylsilyl)butane (CSMSB): A mixture of 1.90 g (14.9 mmol) of 3-butenyltrimethylsilane,[16] 2.0 mL (19.1 mmol) of trichlorosilane, and a pinch of $H_2PtCl_6 \cdot 6H_2O$ was stirred at room temperature for 14 h. Distillation of the resulting mixture under reduced pressure gave 2.13 g (54% yield) of the title compound as a colorless oil; bp 57 °C/2 mmHg; ^{1}H NMR ($CDCl_3$) δ 0.00 (s, 9H), 0.51–0.55 (m, 2H), 1.39–1.47 (m, 4H), 1.54–1.60 (m, 2H); ^{13}C NMR ($CDCl_3$) δ −1.7, 16.2, 24.1, 26.0, 26.3. Found: C, 32.08; H, 6.75%. Calcd for $C_7H_{17}Cl_3Si_2$: C, 31.88; H, 6.50%.

Other Samples: Trichloro(methyl)silane (TCMS in Fig. 1) and TMS were respectively purchased from Shin-Etsu Chemical Co., Ltd. and Tokyo Kasei Kogyo Co., Ltd., and were used without further purification. The preparation of 1,1,1-trimethyltrichlorodisilane [$Cl_3SiSi(CH_3)_3$, MCDS], (trichlorosilyl)(trimethylsilyl)methane [$Cl_3SiCH_2Si(CH_3)_3$, CSMSM], 1-trichlorosilyl-2-trimethylsilylethane [$Cl_3SiCH_2CH_2Si(CH_3)_3$, CSMSE], 1-trichlorosilyl-3-trimethylsilylpropane [$Cl_3SiCH_2CH_2CH_2Si(CH_3)_3$, CSMSP], and (*E*)-1-trichlorosilyl-2-trimethylsilylethene [*trans*-form in $Cl_3SiCH{=}CHSi(CH_3)_3$, CSMSEen] has been reported in previous papers.[17–20]

Measurements. We obtained the binding energies of the Si:1s and 2p core electrons of 1-trifluorosilyl-2-trimethylsilylethane in the vapor phase using a high-resolution monochromator installed in the c branch of the soft X-ray beamline 27SU at the SPring-8 facility[21,22] and a cylindrical-mirror-type electron-energy-analyzer (CMA, Staib ESA-150-D).[23] Detailed results containing the ionic fragmentation pattern have been reported elsewhere.[24]

The Si:2p binding energies of the bridged trihalosilyl-trimethylsilyl molecules in the condensed phase were obtained by using a monochromator installed in the beamline 12A at the Photon Factory facility and a coaxially-symmetric-mirror electron-energy-analyzer.[25–28] The resolution of the electron-energy-analyzer, which was developed by Mase et al.,[26–28] has been greatly improved from that of their former cylindrical-mirror-type electron-energy-analyzers.[19,28,29] Detailed results containing the Auger-photoelectron coincidence spectra will be reported elsewhere.[30] Prior to the measurements in the vapor and condensed phases, the sample was degassed by means of the repeated freeze–pump–thaw method.

The ^{29}Si NMR spectra of the bridged trichlorosilyl-trimethylsilyl molecules and TCMS in $CDCl_3$ were recorded on a JEOL LA-400 spectrometer using TMS as an internal standard.

Computational Method and Procedure

Unless otherwise noted, ab initio and density functional molecular-orbital calculations[15] for the bridged trichlorosilyl-trimethylsilyl molecules were done using the Gaussian 98 program.[31] Since the computationally estimated geometry of an organosilicon molecule is not very sensitive to the basis sets used, but is sensitive to whether a correlated method is employed, all the molecules investigated were optimized at the MP2/6-31G(d) level.[32,33] Since calculation at the HF/6-31G(d) level has been recommended as the minimum model for gauge-independent atomic orbital (GIAO) calculation,[34,35] we calculated the NMR chemical shifts at the HF/6-31G(d)//MP2/6-31G(d) level. The NMR chemical shifts of some molecules were also calculated at the B3LYP/6-311+G(2d,p)//MP2/6-31G(d) level[35] to check the dependence on the computational method.

As noted in a later section, an analysis of the bond order between a Si atom and a neighboring atom (p_k, $k = 1$–4) is useful in our interpretation of the NMR chemical shifts of the bridged trichlorosilyl-trimethylsilyl molecules. However, the analysis attempted with the Gaussian 98 program failed because of too many integration domains.[36] Very recently, the Gaussian 03[37] and NBO[38] programs have provided a powerful means to perform such a bond-order analysis, thus we have estimated the atom–atom overlap-weighted natural-atomic-orbital bond-orders[39] at the HF/6-31G(d)//MP2/6-31G(d) level with these programs.

The ESCA chemical shift can be attributed to two effects: the Coulomb repulsion between a core electron and valence electrons (the initial-state effect[18,40] explained in the next section) and the reorganization (also termed relaxation or polarization) of the valence electrons upon removal of the core electron (the final-state effect[41]). In our estimation of the ESCA chemical shift of the bridged trichlorosilyl-trimethylsilyl molecules, unless otherwise noted, the difference in the Si:2p core-eigenvalue between the two Si sites was calculated and regarded as the difference in the chemical shift due to the initial-state effect. The Si:2p core-eigenvalue was a negative quantity, and the absolute value of the Si[Cl]:2p core-eigenvalue (binding energy [ionization potential] based on Koopmans' theorem[41]) was larger than that of the Si[Me]:2p one as explained in a later section. For comparison, the same computational method as was employed in the calculations of the NMR chemical shifts [HF/6-31G(d)//MP2/6-31G(d)] was used in the calculations of the ESCA chemical shifts. A general basis set [Gen; (3112121/31121)[42] for Si and Cl, (31121/211)[42] for C, and Dunning/Huzinaga full double-zeta[43] for H] was also used [HF/Gen//MP2/6-31G(d) level]. This basis set was chosen to appropriately represent the atomic orbitals of the core electrons.

We also attempted some calculations of the ESCA chemical

shift due to the final-state effect,[20] but found that the amount of the computer read-write-file available to us (20 GB) was insufficient for this purpose except in TCMS [trichloro(methyl)-silane] and TMS with the Gen basis set. However, in bridged trihalosilyl-trimethylsilyl molecules, it is known that the absolute value of the chemical shift due to the final-state effect is likely to be much less than that due to the initial-state effect, and that the chemical shift due to the initial-state effect is a good qualitative measure of the experimental chemical shift.[20]

As noted in a later section, the s-electron density at a nucleus $[|\psi(0)|^2]$ is proportional to the chemical shift in Mössbauer spectroscopy. The ab initio method using Gaussian-type functions is not suitable for any calculations of $|\psi(0)|^2$, because a Gaussian-type function does not have a desired cusp at the nucleus and hence gives a poor representation there.[44] So, by means of the CNDO method,[45] we calculated $|\psi(0)|^2$'s at the two Si sites of the bridged trichlorosilyl-trimethylsilyl molecules.

Results and Discussion

Chemical Shift in ESCA. General Remarks: First, we will briefly describe the cause of the ESCA chemical shift due to the initial-state effect, which was mentioned in the preceding section. This description will be useful for many readers of this paper since our subject extends across two very different fields, ESCA and NMR.

The existence of the ESCA chemical shift can be attributed to the dependence of the electric Coulomb repulsion between a core electron and valence electrons on the chemical environment around the atom containing the core electron (Fig. 2).[40] Let the chemical shift of an isolated Si atom be 0 (Fig. 2a). In Fig. 2b, an electron-accepting Cl atom approaches the Si atom, and the valence electron originally belonging to the Si atom is partly transferred toward the Cl atom. In a simple physical picture, when the transferred charge is $-\delta e$, the potential energy of the core electron of the Si atom changes by $-\delta e \cdot e/r$; hence, the core binding energy (ionization potential) increases by $\delta e \cdot e/r$, which is regarded as the chemical shift from the core binding energy of the isolated Si atom. Here, r denotes the valence shell radius of the Si atom. The situation encountered for a Si atom bonded to an electron-donating CH_3 group is the reverse of one bonded to the electron-accepting Cl atom, and the core binding energy of Si[Me] decreases from that of the isolated Si atom. In this manner, the occurrence and extent of the chemical shift can be understood.

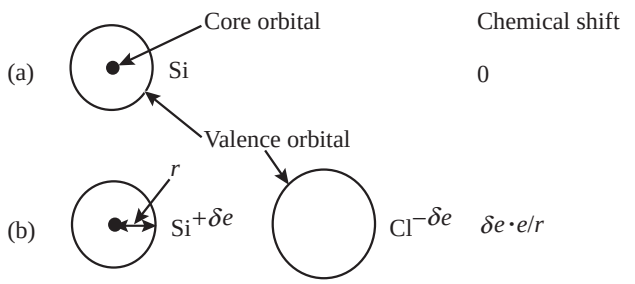

Fig. 2. Schematic explanation of ESCA chemical shift from the core-electron binding energy of an isolated Si atom. (a) Isolated Si atom. The small closed circle and the large open circle denote schematic views of the orbitals of the core and valence electrons, respectively. (b) When an electron-accepting Cl atom approaches a Si atom, part of the valence electron of the Si atom is transferred toward the Cl atom. $-\delta e$ and r respectively denote the transferred charge and the valence shell radius of the Si atom.

Experimental and Computational Results: Let the difference in the Si:2p chemical shift between the Si[Me] and Si[Cl] sites of the bridged trichlorosilyl-trimethylsilyl molecules be ΔE. Here, ΔE is given by the Si[Cl]:2p core binding energy minus the Si[Me]:2p core binding energy. The experimental and computational results of ΔE are summarized in Table 1. For reference, the experimental[46,47] and computational differences in the Si:2p chemical shift between TCMS and TMS (TCMS-TMS) are also listed as ΔE.

Since the ΔE's of CSMSE, CSMSEen, and CSMSEyn (Fig. 1) are similar to one another (Table 1), the bond order between the two C atoms in the bridge connecting the two Si sites (p_{cc}) is unlikely to greatly influence the Si chemical shift. Thus, the effect of the neighboring bridge atom on the Si chemical shift will not be very large in the bridged trichlorosilyl-trimethylsilyl molecules. As shown in Table 1, ΔE for

Table 1. Experimental and Computational Results for ΔE (eV)[a]

Molecule	n	Experimental result[b]	Computational result[c]	
			6-31G(d)	Gen
MCDS	0	2.2[d]	2.60	3.39[e]
CSMSM	1	3.3[d),f]	3.24	4.52
CSMSE	2	3.3[f),g]	3.50	4.85
		(3.2[f),g]) 3.5[d),f]	3.71	5.03)[h]
CSMSP	3	—	3.69	5.10
CSMSB	4	—	3.77	5.21
CSMSPe	5	—	3.83	5.30
TCMS-TMS[i]	∞	4.3[j]	4.08	5.72[e] (7.87)[k]
CSMSEen		—	3.28	4.63
CSMSEyn		—	3.26	4.76

a) ΔE is given by the Si[Cl]:2p core binding energy minus the Si[Me]:2p core binding energy. b) Since a general spectroscopic standard such as TMS in ^{1}H NMR chemical shifts[1,10] is absent in ESCA, calibration of the absolute energy reading is not easy. In fact, the errors inherent in the calibrations are ±3 eV. Accordingly, the absolute binding energies thus obtained are not listed here. However, since the errors inherent in our experiments would simply shift the absolute energy scale while preserving the relative energies, the values of ΔE listed in this table do not actually contain large errors. c) Unless otherwise noted, ΔE due to the initial-state effect. d) Condensed molecule on a Si(111) surface. Because of the improved resolution of the electron-energy analyzer,[26–28] values previously reported for ΔE[19,29] have been revised. e) Values from Ref. 29. f) 1-Trifluorosilyl-2-trimethysilyl molecule. g) Vapor. h) Difference in Si:1s chemical shift. i) Energy difference in Si:2p chemical shift between TCMS and TMS. j) Trifluoro(methyl)silane and TMS vapors. Value from Refs. 46 and 47. k) ΔE due to the initial- and final-state effects.

the Si:2p core binding energy is similar to that for the Si:1s one [footnote h) in Table 1]. ΔE in the condensed phase [footnote d)] is also similar to that in the vapor phase [footnote g)]. The computational ΔE value due to the initial-state effect in TMCS-TMS (5.72 eV) is much larger than ΔE due to the final-state effect (2.15 eV) [ΔE due to the initial- and final-state effects (7.87 eV) minus ΔE due to the initial-state effect (5.72 eV)].

In Fig. 3a, the experimental and computational values of ΔE for MCDS, CSMSM, CSMSE, CSMSP, CSMSB, 1-trichlorosilyl-5-trimethylsilylpentane (CSMSPe), and TCMS-TMS are plotted as a function of the number of CH_2 groups between the two Si sites (n). In TCMS-TMS, the value of n is regarded as ∞. The variation in the computational values according to n is consistent with that in the experimental values. Although ΔE is nearly constant or decreases slightly when going from $n = \infty$ (TCMS-TMS) to 1 (CSMSM), it decreases somewhat rapidly when going from $n = 1$ (CSMSM) to 0 (MCDS).

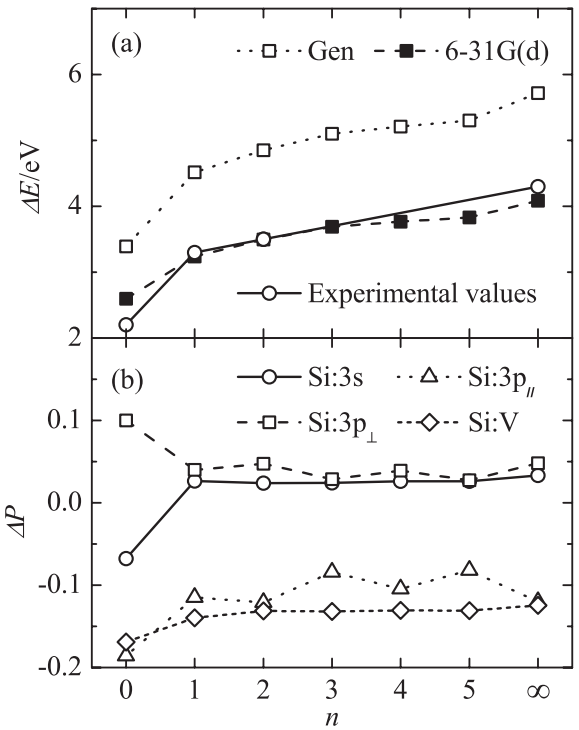

Fig. 3. (a) Plots of experimental and computational values of ΔE versus n in MCDS ($n = 0$), CSMSM ($n = 1$), CSMSE ($n = 2$), CSMSP ($n = 3$), CSMSB ($n = 4$), and CSMSPe ($n = 5$). Here, ΔE is given by the Si[Cl]:2p core binding energy minus the Si[Me]:2p core binding energy. For reference, the difference in Si:2p binding energy between TCMS and TMS is also plotted as ΔE (regarding n as ∞). The open and closed squares refer to the computational results at the HF/Gen//MP2/6-31G(d) and HF/6-31G(d)//MP2/6-31G(d) levels, respectively. The experimental values listed in Table 1 are also plotted (open circles). (b) Plots of the values of ΔP(Si:AO) versus n. Here, AO refers to the Si:3s (open circles), Si:3p$_{//}$ (open triangles), or Si:3p$_{\perp}$ (open squares) orbitals, and ΔP(Si:AO) = P(Si[Me]:AO) − P(Si[Cl]:AO). ΔP(Si:AO) is expressed as a value per orbital. The basis set used in the calculation was 6-31G(d). The ΔP(Si:AO) values for polarization functions, which are related to both Si:3p$_{//}$ and Si:3p$_{\perp}$, are not shown here. The difference in total valence-electron density between Si[Me] and Si[Cl] [ΔP(Si:V)] is also plotted (open diamonds).

Dependence on Bridge: It is important to clarify why ΔE decreases rapidly when going from $n = 1$ to 0 (Fig. 3a). As mentioned in a previous section, the Si:2p chemical shift responsible for ΔE is mainly determined by the magnitude of the Coulomb repulsion between the Si:2p and valence electrons. The magnitude of the Coulomb repulsion responsible for the chemical shift increases with the valence-orbital population at the Si site. The valence-orbital population at the site is affected by the electron-donating and -accepting properties of the atoms (or groups of atoms) nearby. As mentioned in a previous paper,[48] for convenience we classify these electron-donating and -accepting properties according to two factors. The first factor comes from the electron-donating property of the CH_3 group at the Si[Me] site and from the electron-accepting property of the Cl atom at the Si[Cl] site. Owing to these properties, the two Si sites may have considerably different valence-orbital populations and chemical environments in the bridged trichlorosilyl-trimethylsilyl molecules. The second factor comes from the electron-donating property of the $Si(CH_3)_3$ group and from the electron-accepting property of the $SiCl_3$ group; that is, the intramolecular electron migration from $Si(CH_3)_3$ to $SiCl_3$ in MCDS.

Figure 4 shows a schematic representation of the first and second factors in the bridged trichlorosilyl-trimethylsilyl molecules. The two factors increase or decrease the valence-orbital population at each of the two Si atoms, which affects the magnitude of the Si:2p–valence Coulomb repulsion, which in turn changes the Si[Me] and Si[Cl] chemical shifts and hence ΔE. Regarding the first factor, the three CH_3 groups and the three Cl atoms respectively increase and decrease the Si valence-orbital populations owing to their electron-donating and -accepting properties. The difference in valence-orbital population between Si[Me] and Si[Cl] thus appears in CSMSM, CSMSE, CSMSP, CSMSB, CSMSPe, and TCMS-TMS (n = 1–5 and ∞, respectively) as shown in Fig. 4b. As a result, the Si[Me]:2p core electrons are largely destabilized by the Coulomb repulsion against the increasing valence-orbital population at the Si[Me] site. In contrast, the Si[Cl]:2p electrons are stabilized because the valence-orbital population at the Si[Cl] site decreases. ΔE thus appears in CSMSM, CSMSE, CSMSP, CSMSB, CSMSPe, and TCMS-TMS ($n \geq 1$).

On the other hand, the intramolecular electron migration from $Si(CH_3)_3$ to $SiCl_3$ (the second factor) in MCDS ($n = 0$) could have an effect opposite to that of the first factor on the valence-orbital population (Fig. 4a), and hence on ΔE. As a result, the effects of the first and second factors are canceled out in MCDS, leaving ΔE small in total. This cancellation does not occur in the other molecules ($n \geq 1$) because of the greater distance between the two Si sites (Fig. 4b). A large ΔE is thus expected in molecules where the two Si sites are located far apart, but a small ΔE is likely in MCDS where the two Si sites are close together. This qualitative explanation is consistent with the results shown in Fig. 3a.

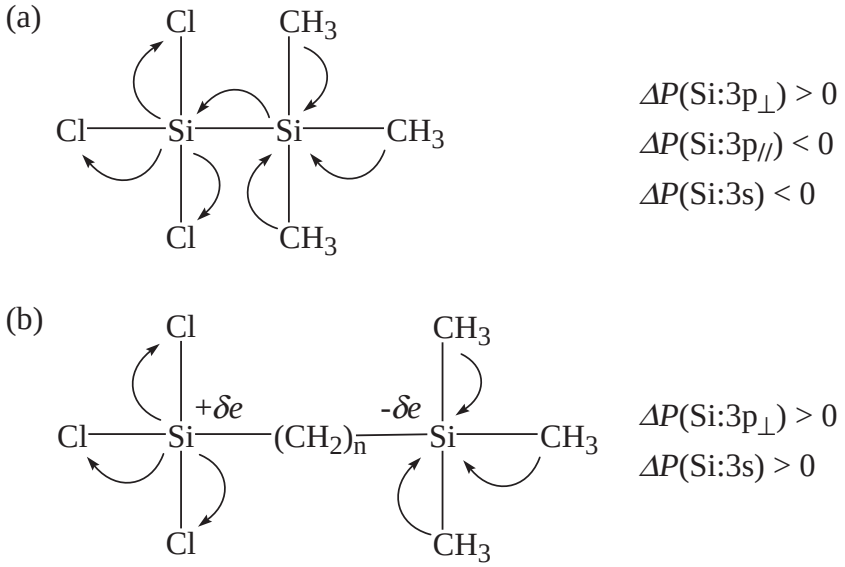

Fig. 4. Schematic representation of the first factor (electron-donating and -accepting properties of CH_3 groups and Cl atoms at Si[Me] and Si[Cl] sites, respectively) and the second factor (intramolecular electron migration from Si[Me] to Si[Cl]). (a) MCDS. (b) CSMSM, CSMSE, CSMSP, CSMSB, and CSMSPe.

Next, we quantitatively examine the explanation given above. At first glance, one might presume that the two factors increase or decrease the *total* valence-electron density at each of the two Si sites, that the increase or decrease affects the Si:2p–valence Coulomb repulsion, and that this influences the Si[Me] and Si[Cl] chemical shifts and hence ΔE. Let the total valence-electron density at a Si[X] site (X = Me or Cl) be P(Si[X]:V), and let P(Si[Me]:V) − P(Si[Cl]:V) be ΔP(Si:V). In Fig. 3b, ΔP(Si:V) is plotted as a function of n. For reference, the difference between P(Si[Me]:V) of TMS and P(Si[Cl]:V) of TCMS is also plotted as ΔP(Si:V) (regarding n as ∞). ΔP(Si:V) is nearly constant for $n \geq 1$. When going from $n = 1$ to 0 (MCDS), $|\Delta P(\text{Si:V})|$ increases and the P(Si[Me]:V) value moves away from the P(Si[Cl]:V) value (Fig. 3b). Thus, the magnitude of the Coulomb repulsion between the Si[Me]:2p electron and P(Si[Me]:V) should then move away from that between Si[Cl]:2p and P(Si[Cl]:V). As a result, when going from $n = 1$ to 0, the Si[Me] chemical shift due to the above Coulomb repulsion should move away from the Si[Cl] one and the Si[Cl]–Si[Me] difference in the chemical shift due to the Coulomb repulsion should increase; that is, ΔE due to the Si[X]:2p–P(Si[X]:V) Coulomb repulsion should increase. However, this expected increase is not consistent with the experimental result that ΔE decreases when going from $n = 1$ to 0 (Fig. 3a). This inconsistency arises because the contributions of individual valence electrons to the Coulomb repulsion are not equal to one another—a valence electron located near the Si:2p electron (an inner-valence electron) shows larger repulsion than another located far from it (an outer-valence electron). Consequently, in our examination of the Coulomb repulsion responsible for ΔE, the valence charge that we have to take as the counterpart for the Si:2p electron cannot be the total valence-electron density at the Si site {P(Si[X]:V)}, but the distribution of each valence electron around the Si site. As the counterpart, an inner-valence electron must be more effective than an outer one.

To give a detailed description of the variation in each valence-electron distribution according to n and to clarify the reason for the small ΔE of MCDS, the valence electrons are allocated in some fractional manner among various atomic orbitals such as Si:3s, Si:3p$_{//}$, and Si:3p$_{\perp}$. Here, the // direction is assumed to point spatially along the σ bond between one Si site and the neighboring Si site or CH_2 group, and the $\perp$ direction is assumed to be perpendicular to the // direction. To allocate the valence electrons in this manner, the concept of gross orbital population[15,31] (P) is useful. In Fig. 3b, the differences in P of the Si:3s, Si:3p$_{//}$, and Si:3p$_{\perp}$ orbitals between the Si[Me] and Si[Cl] sites [ΔP(Si:3s), ΔP(Si:3p$_{//}$), and ΔP-(Si:3p$_{\perp}$), respectively] are plotted as a function of n. Here, ΔP(Si:AO) = P(Si[Me]:AO) − P(Si[Cl]:AO) [AO = 3s, 3p$_{//}$, or 3p$_{\perp}$]. For reference, the population difference between TCMS and TMS is also plotted as ΔP(Si:AO) (regarding n as ∞). The variation in ΔP(Si:AO) according to n is much greater than that in ΔP(Si:V). The values of ΔP(Si:AO) are nearly constant for $n \geq 1$, as is ΔP(Si:V). However, they change rapidly and in various ways when going from $n = 1$ to 0 (MCDS). These rapid changes lead to a rapid change in the magnitude of the Si:2p–valence Coulomb repulsion, and hence these changes lead to the rapid decrease in ΔE when going from $n = 1$ to 0 (Fig. 3a).

The first factor, which comes from the electron-donating and -accepting properties of the CH_3 group and the Cl atom at the Si[Me] and Si[Cl] sites (Fig. 4b), manifests itself in ΔP(Si:3p$_{\perp}$) because the directions of the Si–CH_3 and Si–Cl bonds point nearly along the $\perp$ direction. Owing to the first factor, P(Si[Me]:3p$_{\perp}$) increases and P(Si[Cl]:3p$_{\perp}$) decreases from those of an isolated Si atom, and P(Si[Me]:3p$_{\perp}$) is larger than P(Si[Cl]:3p$_{\perp}$). Therefore, ΔP(Si:3p$_{\perp}$) is larger than zero as shown in Fig. 3b.

In addition, the second factor, which comes from the electron-donating and -accepting properties of the Si(CH_3)$_3$ and $SiCl_3$ groups in MCDS (Fig. 4a), manifests itself in ΔP-

($Si:3p_{//}$) because the intramolecular electron migration from $Si(CH_3)_3$ to $SiCl_3$ takes place along the σ bond. Owing to the second factor, $P(Si[Me]:3p_{//})$ decreases and $P(Si[Cl]:3p_{//})$ increases from those of an isolated Si atom, $P(Si[Me]:3p_{//}) < P(Si[Cl]:3p_{//})$, and $\Delta P(Si:3p_{//}) < 0$ in MCDS (Fig. 3b). To compensate for the intramolecular electron polarization caused by $\Delta P(Si:3p_{//})$ in MCDS, the $\Delta P(Si:AO)$ of the largely spread $Si:3p_{\perp}$ orbitals $[\Delta P(Si:3p_{\perp})]$ increases rapidly when going from $n = 1$ to 0 (MCDS). Accordingly, the change in $\Delta P(Si:V)$ is much less than those in $\Delta P(Si:AO)$ (Fig. 3b).

When going from $n = 1$ to 0 (MCDS), $|\Delta P(Si:3p_{\xi})|$ ($\xi = //$ or $\perp$) increases rapidly (Fig. 3b). Thus, the difference in the $Si:3p_{\xi}$ valence-orbital population between the Si[Me] and Si[Cl] sites then increases rapidly and $P(Si[Me]:3p_{\xi})$ moves away from $P(Si[Cl]:3p_{\xi})$. As a result, in MCDS the magnitude of the Si:2p–$Si:3p_{\xi}$ Coulomb repulsion at the Si[Me] site should be very different from that at the Si[Cl] site, and the Si[Me] chemical shift due to the above Coulomb repulsion should be very different from the Si[Cl] one. Thus, the Si[Cl]–Si[Me] difference in the chemical shift due to the Coulomb repulsion should increase when going from $n = 1$ to 0; that is, ΔE due to the Si:2p–$Si:3p_{\xi}$ Coulomb repulsion should increase. However, this expected increase is not consistent with the experimental result where ΔE decreases when going from $n = 1$ to 0 (Fig. 3a). This inconsistency suggests that ΔE is not mainly determined by the magnitude of the Coulomb repulsion of the Si:2p electron against the $Si:3p_{\xi}$ electron, but by that against the other valence electron: i.e., against the Si:3s electron, which is located closer to Si:2p than $Si:3p_{\xi}$ is.[49]

$\Delta P(Si:3s)$ is left for us to examine the variation according to n and to determine the relationship with ΔE. Both the first and second factors (Fig. 4) affect $\Delta P(Si:3s)$. In fact, as shown in Fig. 3b, $\Delta P(Si:3s)$ is larger than zero and nearly constant for $n \geq 1$, as is $\Delta P(Si:3p_{\perp})$ (the first factor), and when going from $n = 1$ to 0 (MCDS) it decreases rapidly and becomes a negative quantity along with $\Delta P(Si:3p_{//})$ in MCDS (the second factor). The variation in $\Delta P(Si:3s)$ according to n is fully parallel to the qualitative explanation given in Fig. 4.

The distribution of the Si:3s electron overlaps with that of the Si:2p electron more fully than the distribution of the $Si:3p_{\xi}$ electron does, and the average distance between the Si:3s and Si:2p electrons is less than that between the $Si:3p_{\xi}$ and Si:2p electrons.[49] Accordingly, the Si:3s valence electron should show greater Coulomb repulsion against the Si:2p core electron than the $Si:3p_{\xi}$ electron does; thus, $\Delta P(Si:3s)$ will affect the inter-site difference in the magnitude of the Coulomb repulsion more than $\Delta P(Si:3p_{\xi})$ does. As a result, the magnitude of the Coulomb repulsion between the Si:3s and Si:2p electrons mainly determines the chemical shift responsible for ΔE; thus, $\Delta P(Si:3s)$ strongly influences ΔE. Therefore, because the Si:3s–Si:2p Coulomb repulsion changes greatly owing to the large change in $\Delta P(Si:3s)$ when going from $n = 1$ to 0, ΔE decreases rapidly (Fig. 3a). The intramolecular electron polarization induced by the $\Delta P(Si:3s)$ in MCDS is compensated for by the $\Delta P(Si:3p_{\perp})$. This interpretation is consistent with the experimental and computational results.

The results presented so far indicate that the chemical shift of the bridged trichlorosilyl-trimethylsilyl molecules mainly reflects the population of the Si:3s orbital: that is, the electronic environment within a mean radius of 1.168 Å[49] of the Si site. A similar result was reported for C:1s ESCA chemical shifts, which reflect the spherically averaged electron density on a sphere with radius ≈0.7 Å centered at the carbon atom concerned.[50] However, it is very difficult to represent ΔE explicitly as a function of $\Delta P(Si:3s)$. When going from $n = 1$ to 0, intramolecular electron polarization caused by a change of $\Delta P(Si:AO)$ is avoided through compensation by the other $\Delta P(Si:AO)$'s so as to stabilize the molecule, and the change in $\Delta P(Si:V)$ is much less than that in $\Delta P(Si:AO)$.

In Fig. 4, the first factor, which comes from the electron-donating and -accepting properties of the CH_3 group and the Cl atom at the Si[Me] and Si[Cl] sites, manifests itself in $\Delta P(Si:3p_{\perp}) > 0$ and $\Delta P(Si:3s) > 0$ for $n \geq 1$ (Fig. 4b). Since $\Delta P(Si:3p_{//})$ should be negative so as to avoid intramolecular electron polarization, the electron migration from Si[Me] to the bridge and from the bridge to Si[Cl] along its σ bond is not negligible for $n \geq 1$. In total, $\Delta P(Si:V) < 0$ for $n \geq 1$ (Fig. 3b). In addition, the second factor, which comes from the electron-donating and -accepting properties of the $Si(CH_3)_3$ and $SiCl_3$ groups, manifests itself in $\Delta P(Si:3p_{//}) < 0$ and $\Delta P(Si:3s) < 0$ for $n = 0$ (Fig. 4a). To compensate for intramolecular electron polarization, $\Delta P(Si:3p_{\perp})$ $(n = 0) > \Delta P(Si:3p_{\perp})$ $(n \geq 1) > 0$. In total, $\Delta P(Si:V) < 0$ for $n = 0$. Because of $\Delta P(Si:V)$ $(n = 0) < \Delta P(Si:V)$ $(n \geq 1) < 0$ (Fig. 3b), the second factor $[\Delta P(Si:3p_{//}) < 0$ and $\Delta P(Si:3s) < 0]$ is likely to play an important role for $n = 0$.

Chemical Shift in NMR. General Remarks: First, we will briefly explain the principles necessary to understand NMR chemical shifts caused by magnetic interaction so that all readers can easily understand this part of our paper, again since our subject extends over two very different fields, ESCA and NMR. The NMR chemical shift can mainly be attributed to three effects—the diamagnetic effect from the electrons of the atom that contains the nucleus in question (the local diamagnetic effect), the paramagnetic effect from the electrons of the atom that contains the nucleus in question (the local paramagnetic effect), and the effect from groups of the atoms that form the rest of the molecule (the remote effect).[1,51]

The local diamagnetic effect arises from the ability of the applied magnetic field (H_0) to generate a circulation of charge in the ground-state electron distribution of the atom that contains the nucleus in question. The circulation produces a magnetic field that opposes H_0, and thus, the nucleus in question feels a total magnetic field (local field, H_{local}) less than H_0. This phenomenon is called shielding of the nucleus. H_{local} is given by

$$H_{local} = H_0 + H' = (1 - \sigma_d)H_0, \quad (1)$$

where $H' < 0$ and $\sigma_d = -H'/H_0 > 0$. σ_d is called the local diamagnetic contribution to the shielding constant.

The NMR experiment uses resonance electromagnetic-wave absorption by nuclei exposed to H_{local}.[51] The energy separation between the α and β spin states of a spin-1/2 nucleus such as ^{29}Si is $\gamma h H_{local}$, and the resonance absorption occurs when the resonance condition $h\nu = \gamma h H_{local}$ is fulfilled. Here, γ denotes the magnetogyric ratio of the nucleus in question. The frequency of the resonant electromagnetic wave (ν) is observed in the NMR experiment.

In the local diamagnetic contribution, as well as the other contributions mentioned later, the ν is conventionally expressed in terms of an empirical quantity called the "NMR chemical shift δ," which is related to the difference between the ν of the nucleus of interest and that of a reference standard (ν_0). The amount of δ is expressed in ppm:

$$\delta = 10^6(\nu - \nu_0)/\nu_0 = 10^6(\sigma_0 - \sigma)/(1 - \sigma_0) \approx 10^6(\sigma_0 - \sigma), \quad (2)$$

where σ and σ_0 denote the total shielding constant of the nucleus of interest and that of the reference standard, respectively. σ is given by the sum of σ_d and the other shielding constants mentioned later. From Eqs. 1 and 2, the local diamagnetic contribution, designated here as δ_d, to δ is nearly equal to $10^6(H' - H_0')/H_0$, where H_0' denotes H' of the reference standard. δ is given by the sum of δ_d and the other chemical shifts mentioned later.

σ_d is a positive quantity as mentioned above and is broadly proportional to the total electron density of the atom containing the nucleus in question [P(Si:V) in the present case].[1,51] It follows that σ_d increases if P(Si:V) increases because of the effect of a nearby electron-donating atom (or a group of atoms such as a CH_3 group). This increase in σ_d translates into a decrease in δ_d (Eq. 2). That is, as the electron-donating property of the nearby atom or group increases and P(Si:V) increases, δ_d decreases. We can thus write the equation of δ_d as

$$\delta_d = -C_1\{P(\text{Si:V}) - P_0(\text{Si:V})\}, \quad (3)$$

where C_1 is a positive constant quantity and P_0(Si:V) denotes P(Si:V) of the reference standard.

The local paramagnetic effect arises from the ability of the applied field to force the electrons of the atom in question to circulate through the molecule by making use of orbitals that are unoccupied in the ground state.[1,51] As reported by Prosser and Goodman,[52] it is reasonable to consider the local paramagnetic contribution (δ_p) to δ of ^{29}Si in the bridged trichlorosilyltrimethylsilyl molecules to be primarily a function of four parameters: (1) P(Si:V), (2) the bond orders between the Si atom and the neighboring four atoms (p_k, k = 1–4), (3) the average energy difference between the ground and excited states (δE), and (4) the valence-electron density of the neighboring four atoms (P_k, k = 1–4).[52] We may write the equation of δ_p as

$$\delta_p = f[P(\text{Si:V}), p_k, P_k]/\delta E, \quad (4)$$

where $f[P$(Si:V), p_k, $P_k]$ denotes a function of P(Si:V), p_k and P_k.[52]

The remote effect arises from electron circulation induced in nearby groups of atoms.[1,51] For example, the ^{1}H chemical shifts of the set of ethane (H_3C–CH_3), ethylene (H_2C=CH_2), and acetylene (HC≡CH) are interesting.[1] According to a simple intuitive view, the $\delta(^1H)$ value should increase or decrease as the bond order between the two C atoms increases. In reality, however, the $\delta(^1H)$ value increases in the order H_3C–CH_3 < HC≡CH < H_2C=CH_2. This irregular order is attributed to the remote effect caused by electron circulation in the bond between the two C atoms.[1]

Experimental and Computational Results: The experimental and computational results for $\delta(^{29}Si)$ of the bridged trichlorosilyl-trimethylsilyl molecules are summarized in Table 2 together with those of TCMS (using TMS as the reference standard). Let the difference in δ between the Si[Me] and Si[Cl] sites be $\Delta\delta$. Here, $\Delta\delta$ is given by the δ at the Si[Cl] site {δ(Si[Cl])} minus the δ at the Si[Me] site {δ(Si[Me])}. The experimental and computational results for $\Delta\delta$ are also shown in Table 2. For reference, the experimental and computational differences in $\delta(^{29}Si)$ between TCMS and TMS (TCMS-TMS) are also listed as $\Delta\delta$. In Fig. 5a, the $\Delta\delta$ values of MCDS, CSMSM, CSMSE, CSMSP, CSMSB, CSMSPe, and TCMS-TMS are plotted as a function of n. In TCMS-TMS, the value of n is regarded as ∞, as in the ESCA chemical shift.

In Table 2 and Fig. 5a, the variation in the computational values [HF/6-31G(d)//MP2/6-31G(d) level] according to the length and the bond order p_{cc} of the bridge connecting the two Si sites qualitatively agrees with that in the experimental values. Although the quantitative agreement between the experimental values and the computational values at the B3LYP/6-311+G(2d,p)//MP2/6-31G(d) level is improved from that at the HF/6-31G(d)//MP2/6-31G(d) level, it is still unsatisfactory. However, since sufficient qualitative agreement between the experimental and computational values at the HF/6-31G(d)//MP2/6-31G(d) level was achieved, its computational values will be used in the discussion given below.

In Fig. 5a, $\Delta\delta$ is nearly constant for $n \geq 1$. When going from n = 1 (CSMSM) to 0 (MCDS), $\Delta\delta$ increases although ΔE decreases as explained in a previous section (Fig. 3a); that is, the ^{29}Si NMR chemical-shift values of the two Si sites then move away from each other, although the Si:2p ESCA chemical-shift values approach each other. We suggest a reason for this contrast between the ESCA and NMR chemical shifts in the next section.

The values of δ and $\Delta\delta$ for CSMSE [Cl_3Si–CH_2–CH_2–$Si(CH_3)_3$], CSMSEen [Cl_3Si–CH=CH–$Si(CH_3)_3$], and CSMSEyn [Cl_3Si–C≡C–$Si(CH_3)_3$] rapidly decrease in that order (Table 2). The features of the three δ values are very different from those of the ^{1}H chemical shifts of H_3C–CH_3, H_2C=CH_2, and HC≡CH described in the preceding section. In contrast to their irregular ^{1}H-chemical-shift variation that the remote effect induces, the ^{29}Si NMR chemical shift of CSMSE, CSMSEen, and CSMSEyn systematically decreases as the bond order p_{cc} increases. Judging from this contrast, it seems that the remote effect would make only small contributions to the values of $\delta(^{29}Si)$ for the bridged trichlorosilyl-trimethylsilyl molecules. Therefore, we will hereafter take only the local diamagnetic and paramagnetic effects into account in our interpretation of the δ's and $\Delta\delta$'s of these molecules. The possibility of the remote effect contributing to δ and $\Delta\delta$, however, is explained in the Supporting Information.

Dependence on Bridge: When the bond order p_{cc} increases among CSMSE, CSMSEen, and CSMSEyn, there is a striking contrast between the variation in the NMR chemical shift and that in the ESCA chemical shift. As noted in a previous section, p_{cc} does not strongly affect the ESCA chemical shift of the Si atom of these molecules, and the effect of the neighboring bridge atom on the Si ESCA chemical shift is not very large. In contrast, as mentioned in the preceding section, p_{cc} has a large influence on the Si NMR chemical shift. The effect of the neighboring bridge atom on the Si NMR chemical shift is therefore very large. These results show that the ESCA

Table 2. Experimental and Computational Results for δ (ppm) and $\Delta\delta$ (ppm)

Molecule	n	Experimental result			Computational result[a)]		
		δ		$\Delta\delta$[b)]	δ		$\Delta\delta$[b)]
		Si[Cl]	Si[Me]		Si[Cl]	Si[Me]	
MCDS	0	18.76	−5.67	24.43	62.04	−5.03	67.07
					(41.78	−5.57	47.35)[c)]
CSMSM	1	10.25	0.29	9.96	44.43	1.88	42.55
					(32.44	−0.24	32.68)[c)]
CSMSE	2	13.67	3.95	9.72	45.45	4.95	40.50
CSMSP	3	12.26	0.99	11.27	44.24	2.71	41.53
CSMSB	4	13.03	1.37	11.66	44.41	2.76	41.65
CSMSPe	5	—	—	—	44.53	2.75	41.78
TCMS-TMS	∞	13.01[d)]	0[e)]	13.01[f)]	41.72[d)]	0[e)]	41.72[f)]
					(33.57[d)]	0[e)]	33.57[f)])[c)]
CSMSEen		−4.44	−5.32	0.88	24.46	−2.72	27.18
CSMSEyn		—	—	—	1.49	−8.21	9.70

a) Unless otherwise noted, HF/6-31G(d)//MP2/6-31G(d). b) $\Delta\delta = \delta$(Si[Cl]) − δ(Si[Me]). c) B3LYP/6-311+G(2d,p)//MP2/6-31G(d). d) δ of TCMS. e) δ of TMS. Reference standard. f) Difference in δ between TCMS and TMS.

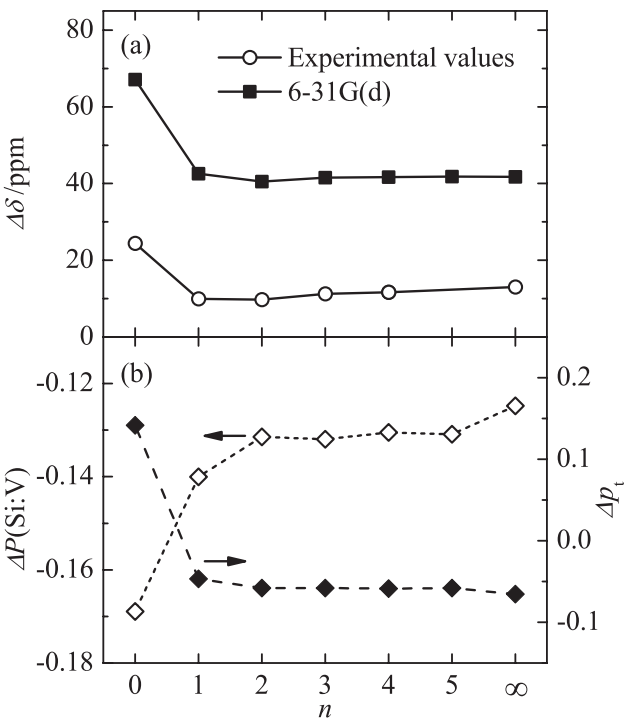

Fig. 5. (a) Plots of experimental and computational values of $\Delta\delta$ (open circles and closed squares, respectively) versus n in MCDS ($n = 0$), CSMSM ($n = 1$), CSMSE ($n = 2$), CSMSP ($n = 3$), CSMSB ($n = 4$), and CSMSPe ($n = 5$). Here, $\Delta\delta = \delta$(Si[Cl]) − δ(Si[Me]). For reference, the difference in δ between TCMS and TMS (TCMS-TMS) is also plotted as $\Delta\delta$ (regarding n as ∞). The calculations of $\Delta\delta$ were performed at the HF/6-31G(d)//MP2/6-31G(d) level. (b) Plots of ΔP(Si:V) and Δp_t versus n (open and closed diamonds, respectively). Here, ΔP(Si:V) = P(Si[Me]:V) − P(Si[Cl]:V) and $\Delta p_t = p_t$(Si[Me]) − p_t(Si[Cl]). In the plot of ΔP(Si:V), the vertical scale is enlarged from that in Fig. 3b.

chemical shift reflects the electronic environment of a small space around the Si atom, while the NMR chemical shift reflects the environment of a larger space.

As mentioned, δ and $\Delta\delta$ of CSMSE, CSMSEen, and CSMSEyn (Table 2) depend largely on the bond order p_{cc}. Which of P(Si:V), p_k, P_k, and δE involved in Eqs. 3 and 4 depend on p_{cc} and are responsible for the changes in δ and $\Delta\delta$ of these molecules? P_k in Eq. 4 does not strongly influence δ_p,[52] and the area with which P(Si:V) in Eqs. 3 and 4 is concerned is located far from the bridge inter-carbon bond whose bond order is p_{cc}. So, judging from Eqs. 3 and 4, the dependence of δ and $\Delta\delta$ on p_{cc} in these cases comes from the dependence of p_k ($k = 1$–4) and/or δE on p_{cc}. In fact, p_k increases as p_{cc} increases as shown in the Supporting Information. Thus, it is reasonable to consider p_k from Eq. 4 (local paramagnetic effect) as being responsible for the changes in δ and $\Delta\delta$ among CSMSE, CSMSEen, and CSMSEyn. Furthermore, δE from Eq. 4 may decrease when a π bond is formed between the two C atoms in the bridge.[53] Note, however, that δE denotes the *average* energy difference between the ground and excited states, so the estimation of δE is not so easy.[1] In any event, through the local paramagnetic effect (Eq. 4), δ and $\Delta\delta$ are likely to reflect the electronic environment near the neighboring atoms in addition to that at the Si site, although the remote effect makes only a small contribution to the δ(^{29}Si)'s as explained in the preceding section. Thus, the ^{29}Si NMR chemical shift reflects the electronic environment within a radius of more than 1.875 Å (Si–C bond length of TMS)[54] of the Si site, although the ESCA chemical shift is considered to reflect the electronic environment within a mean radius of 1.168 Å[49] of the Si site (see a previous section).

In MCDS, CSMSM, CSMSE, CSMSP, CSMSB, CSMSPe, and TCMS-TMS ($n = 0$–∞), the dependence of $\Delta\delta$ on n (Fig. 5a) cannot be interpreted easily because the explicit form of Eq. 4, which is given in Ref. 52, is complex. Accordingly, we assume here, as in Ref. 52, that δE is nearly constant in the series of molecules and that it is possible to rewrite Eq. 4 in

terms of a single P(Si:V) for these molecules. As mentioned, P_k does not have a large influence on δ_p.[52] Then, δ is given by

$$\delta = \delta_d + \delta_p = C_2\{P(\text{Si:V}) - P_0(\text{Si:V})\}, \quad (5)$$

where C_2 is a constant for the series of molecules mentioned above. After all, the ^{29}Si chemical shift of these molecules is regarded as reflecting the total valence-electron density at the Si site. From Eq. 5, $\Delta\delta$ is given by

$$-\Delta\delta = C_2\Delta P(\text{Si:V}). \quad (6)$$

The negative sign in Eq. 6 comes from the definitions $\Delta\delta = \delta(\text{Si[Cl]}) - \delta(\text{Si[Me]})$ and $\Delta P(\text{Si:V}) = P(\text{Si[Me]:V}) - P(\text{Si[Cl]:V})$.

In MCDS, CSMSM, CSMSE, CSMSP, CSMSB, CSMSPe, and TCMS-TMS, $\Delta\delta$ is a positive nearly-constant quantity for $n \geq 1$, and $\Delta\delta$ increases when going from $n = 1$ to 0 (Fig. 5a). ΔP(Si:V) is a negative nearly-constant quantity for $n \geq 1$, and ΔP(Si:V) decreases when going from $n = 1$ to 0 (Fig. 5b). Thus, $-\Delta\delta$ changes on a parallel with ΔP(Si:V), and Eq. 6 is qualitatively consistent with the experimental and computational results. Since P(Si:V) depends on a larger electronic environment around the Si site than P(Si:3s) does, the above result (Fig. 5) does not contradict our claim that the ^{29}Si NMR chemical shift reflects a larger electronic environment than the ESCA chemical shift does.

It is necessary to critically examine Eqs. 5 and 6 and the above-mentioned result (Fig. 5). When dealing with members of a limited type of molecules, correlation between the NMR chemical shift and charge may appear to be relevant, but this may be only by accident. Prosser and Goodman also emphasized that their final equation for δ_p, which leads to Eq. 5, is a limiting case for certain specific compounds.[52] Therefore, we next examine the dependence of the total bond order around the Si site $\{p_t(\text{Si[X]}),\ \text{X} = \text{Me or Cl}\}$ on n, because δ_p is expected to depend linearly on the bond order.[52] Let the difference in the computational p_t(Si[X]) value between the two Si sites be Δp_t, which is given by $p_t(\text{Si[Me]}) - p_t(\text{Si[Cl]})$. Δp_t decreases rapidly when going from $n = 0$ to 1, and is a nearly-constant quantity for $n \geq 1$ (Fig. 5b). Thus, p_t(Si[Me]) and p_t(Si[Cl]) approach each other when going from $n = 0$ to 1, and so $\Delta\delta$ changes on a parallel with Δp_t (Figs. 5a and 5b). Since p_t(Si[X]) depends on a larger electronic environment around the Si site than P(Si[X]:3s) does, this result also supports our view that the ^{29}Si NMR chemical shift reflects a larger electronic environment than the ESCA chemical shift does. Even if our premise that P_k does not have a large influence on δ_p is not valid, it does not lead to a serious problem concerning our conclusion, because the ^{29}Si NMR chemical shift then reflects the electronic environment of a very large space with which P_k is concerned. Although we assumed that δE is nearly constant in the series of molecules, δE denotes the *average* energy difference between the ground and excited states, so the estimation of δE is not so easy.[1] However, δE basically seems to depend on the electronic structure of the whole molecule (a still larger space).

From the results so far presented, we consider the ^{29}Si NMR chemical shift of the bridged trichlorosilyl-trimethylsilyl molecules to reflect the electronic environment within a radius of more than 1.875 Å (Si–C bond length of TMS)[54] of the Si site. In contrast, as described in a previous section, the ESCA chemical shift is considered to mainly reflect the electronic environment within a mean radius of 1.168 Å[49] of the Si site. The ESCA chemical shift is sensitive to the distribution of each valence electron, but the NMR chemical shift is insensitive to this and depends on the whole electron environment over a large space around the Si site.

The difference in the effective electronic environment between the ESCA and NMR chemical shifts may be related to the fact that the inner-valence-electron distribution is overlapped with the core electron distribution (ESCA), but the electronic current generated by H_0 (the external magnetic field) is not located very closely to the nuclei (NMR). In a simple physical picture (Fig. 6), the external magnetic field acts on molecular electrons from outside of the molecule in NMR, so it preferentially induces outer-valence-electron circulation near the molecular surface. The inner-valence electrons are then shielded from the external field. The interaction of the induced molecular-surface electron-circulation with the central nucleus of an atom is so weak that the value of δ is expressed

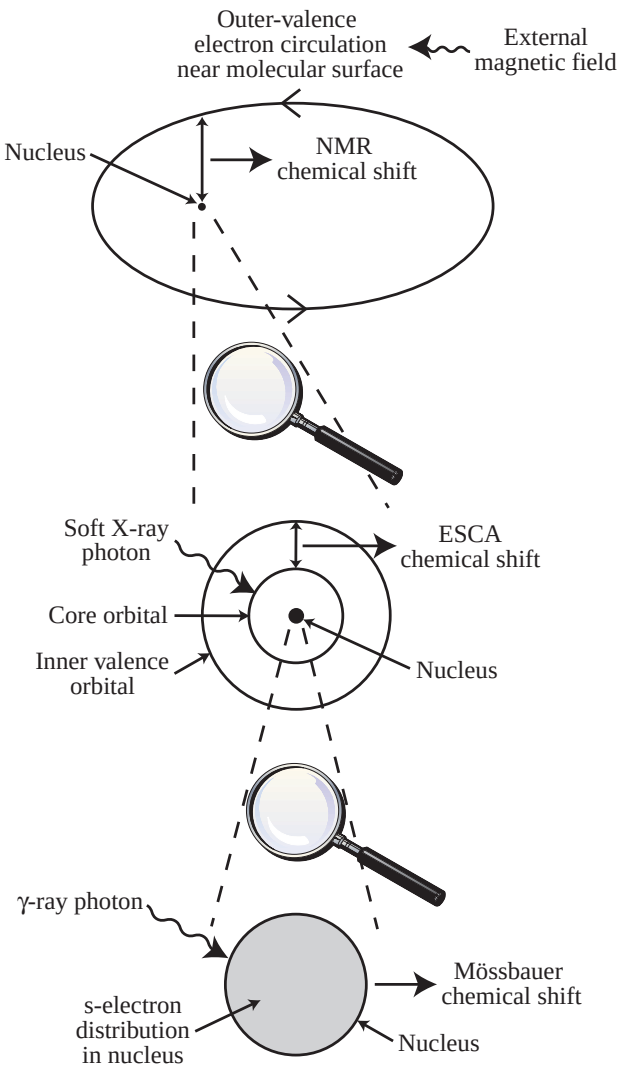

Fig. 6. Schematic comparison of NMR, ESCA, and Mössbauer chemical shifts.

in ppm. In contrast, the interaction energy in ESCA is much greater than that in NMR, because a soft X-ray photon penetrates the valence electron cloud to eject a core electron that is localized near a nucleus and interacts with nearby inner-valence electrons (Fig. 6). In ESCA, the interaction between the core and inner-valence electrons thus takes place in a small space. Consequently, the spatial ranges of the electronic environment affecting the chemical shifts in ESCA and NMR are small and large, respectively.

Another Chemical Shift. In this paper, we have so far discussed the term "chemical shift" as it is used in two types of spectroscopy, ESCA and NMR. Before concluding this paper, we want to point out that the term "chemical shift" is also used in Mössbauer spectroscopy.[1,55] This phenomenon was first observed in 1960,[56] and was called an "isomeric shift" in Mössbauer's Nobel lecture in 1961.[57] Its IUPAC name is now "isomer shift,"[58] but it is also called a "chemical shift."[1,59–61] The circumstances of the naming are not given in the literature.[56,58] Walker et al.[61] wrote, "Unfortunately, the phrase "chemical shift" has been used to describe Mössbauer isomer shifts," but the shift in Mössbauer spectroscopy is affected by the *chemical* environments (oxidation, bonding arrangement, and so on) around the atomic sites as are the chemical shifts in ESCA and NMR.

Figure 7 provides a schematic explanation of the Mössbauer chemical shift from the transition energy of an imaginary point nucleus. The non-zero volume of a nucleus and the electron density due to s-electrons within it induce nucleus–electron electric Coulomb interaction, which alters the nuclear energy levels. We assume that the Coulomb potential within the nucleus is constant and equal to Ze/R, where R and Z stand for the nuclear radius and the atomic number, respectively. Then, the Coulomb-interaction energy ($\mathcal{E}$) is given by[55]

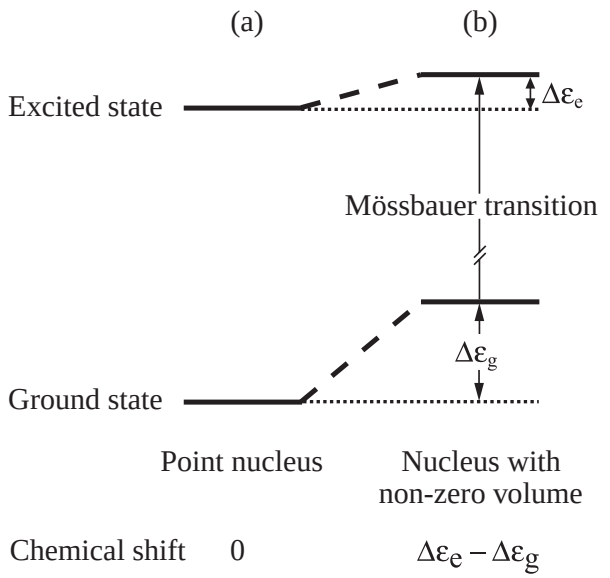

Fig. 7. Schematic explanation of the Mössbauer chemical shift from the transition energy of an imaginary point nucleus. (a) Nuclear excited and ground states of an imaginary point nucleus. (b) Those of a nucleus with non-zero volume and $R_e < R_g$.

$$\mathcal{E} = -e|\psi(0)|^2 \int_0^R 4\pi r^2 (Ze/R)\mathrm{d}r, \tag{7}$$

where $|\psi(0)|^2$ denotes the s-electron density at the nucleus and is assumed to be constant when $r < R$. The energy difference from the imaginary point nucleus ($\Delta\mathcal{E}$) is then given by[1,55]

$$\Delta\mathcal{E} = -e|\psi(0)|^2 \left\{ \int_0^R 4\pi r^2 (Ze/R)\mathrm{d}r - \int_0^R 4\pi r^2 (Ze/r)\mathrm{d}r \right\} = (2/3)\pi Ze^2 R^2 |\psi(0)|^2. \tag{8}$$

In Mössbauer spectroscopy, the transition energy from the ground state to an excited state of the nucleus is observed through the resonance absorption of γ-rays. The transition energy of the nucleus with radius R is different from that of the point nucleus, if R in the excited state (R_e) is different from that in the ground state (R_g). The transition-energy difference is given by $\Delta\mathcal{E}_e - \Delta\mathcal{E}_g$ (Eq. 9), where $\Delta\mathcal{E}_e$ and $\Delta\mathcal{E}_g$ respectively refer to the energy differences from the point nucleus for the excited and ground states and are estimated by Eq. 8:

$$\Delta\mathcal{E}_e - \Delta\mathcal{E}_g = (2/3)\pi Ze^2 (R_e{}^2 - R_g{}^2)|\psi(0)|^2, \tag{9}$$

which is the Mössbauer chemical shift from the transition energy of the point nucleus. Usually, instead of Eq. 9, the Mössbauer chemical shift is expressed as the transition-energy difference between a sample and a reference standard (Δ). In this case, Δ is given by

$$\Delta = (\Delta\mathcal{E}_e - \Delta\mathcal{E}_g) - (\Delta\mathcal{E}_{e0} - \Delta\mathcal{E}_{g0}), \tag{10}$$

where the subscript 0 refers to the reference standard. From Eqs. 8–10, Δ can be expressed as[1,55]

$$\Delta = (2/3)\pi Ze^2 (R_e{}^2 - R_g{}^2)\{|\psi(0)|^2 - |\psi(0)|_0{}^2\}, \tag{11}$$

where R_e and R_g of the reference standard are assumed to be the same as those of the sample.

If R_e is less than R_g as in ^{57}Fe,[1,55] Δ increases as $|\psi(0)|^2$ decreases, as derived from Eq. 11. The value of $|\psi(0)|^2$ is affected by the chemical environment around the nucleus. In ^{57}Fe, the greater the number of d electrons present, the more the nucleus is shielded from the s electrons. This forces the s cloud to expand, reducing $|\psi(0)|^2$, and increasing Δ in Eq. 11.[1,60,61] From this, the chemical shift in Mössbauer spectroscopy can be used to discern different chemical environments around nuclei, allowing us to discriminate between different oxidation states and bonding arrangements (that is, different chemical environments) in unknown samples. Thus, the Mössbauer chemical shift reflects the electronic environment [$|\psi(0)|^2$] within the nucleus in question ($< R$); that is, within a radius of 3.01 fm (nuclear radius of Si)[62] (Fig. 6).

It is interesting that linear correlations have been found between ESCA chemical shifts and Mössbauer chemical shifts for compounds of Fe and Sn.[1] However, it is regrettable that to the best of our knowledge no Mössbauer spectrum originating from a Si atom in a molecule has been reported.

As given in Eq. 11, $|\psi(0)|^2$ is proportional to the Mössbauer chemical shift. Let the difference in the computational $|\psi(0)|^2$ value between the two Si sites of the bridged trichlorosilyltrimethylsilyl molecules be $\Delta|\psi(0)|^2$. In the Supporting Information, the values of $\Delta|\psi(0)|^2$ for MCDS, CSMSM, CSMSE, CSMSP, CSMSB, CSMSPe, and TCMS-TMS are plotted as a

function of n. There, the variation in $\Delta|\psi(0)|^2$ nearly parallels that of ΔE. If the Si Mössbauer chemical shifts of these molecules are obtained, we expect that their variation will be found to nearly parallel that of the corresponding ESCA chemical shifts according to the length of the bridge between the two Si sites.

Conclusion

We have presented a detailed examination of the relationship between the chemical shifts in ESCA and NMR for the Si[Cl] and Si[Me] sites of bridged trichlorosilyl-trimethylsilyl molecules. We have shown that the ESCA chemical shift of a Si site mainly depends on the electronic environment within a mean radius of 1.168 Å of the nucleus and that the NMR chemical shift reflects the electronic environment within a radius of more than 1.875 Å. On the other hand, the Mössbauer chemical shift is affected by the electronic environment within a radius of 3.01 fm. Since the chemical environment around the atom of interest influences the electronic environment in each of these three spatial ranges, using the prefix "chemical" for the shifts observed in the three forms of spectroscopy is appropriate. However, it is important to understand that the chemical environment induces the three chemical shifts in three different ways through the electronic environment in these different spatial ranges around the nucleus.

SN expresses his sincere thanks to Professor Nobuyoshi Hosoito of Nara Institute of Science and Technology (NAIST) and Professor Tatsuo Kamimori of Ehime University for their valuable discussion. SN also thanks the members of the research team for SPring-8 soft X-ray photochemistry (especially Professor Kazumasa Okada of Hiroshima University, Professor Toshio Ibuki of Kyoto University of Education, and Dr. Isao H. Suzuki of AIST) for their kind help and the SPring-8 facility staff (especially Dr. Yusuke Tamenori) for his assistance during the ESCA vapor-phase experiments. In this study, the experiments on the ESCA chemical shift in the vapor phase were carried out with the approval of the Japan Synchrotron Radiation Research Institute (JASRI) as a Nanotechnology Support Project of the Ministry of Education, Culture, Sports, Science and Technology (Proposal Nos. 2002A0029-NS1-np, 2002B0101-NS1-np, 2003A0023-NS1-np, and 2004A0055-NSb-np-Na/BL-No.27SU). SN also thanks Professor Kazuhiko Mase, Dr. Eiichi Kobayashi, and Dr. Akira Nambu of the Institute of Materials Structure Science for their kind help and the Photon Factory facility staff for their assistance during the ESCA condensed-phase experiments. In this study, the experiments on the ESCA chemical shift in the condensed phase were performed under the approval of the Photon Factory Program Advisory Committee (Proposal Nos. 2002G114, 2004G017, 2004G026, and 2004G301). SN and UN thank the Research Center for Computational Science, Okazaki Research Facilities, the National Institutes of Natural Sciences for the use of the Fujitsu VPP5000 and NEC SX-7 computers and the Library Programs Gaussian 98 and Gaussian 03.

Supporting Information

Description of a possibility of the remote effect contributing to δ and $\Delta\delta$; total atom–atom overlap-weighted natural-atomic-orbital bond-orders around Si[Me] and Si[Cl] atoms of CSMSE, CSMSEen, and CSMSEyn; and computational results for $\Delta|\psi(0)|^2$. This material is available free of charge on the web at http://www.csj.jp/journals/bcsj/.

References

1 R. S. Drago, *Physical Methods for Chemists*, 2nd ed., Saunders College Publishing, Ft. Worth, **1992**, Chaps. 7, 15, and 16.

2 S. G. Levine, *J. Chem. Educ.* **2001**, *78*, 133. Before the first observation of the chemical shift in NMR, Knight shift in the NMR frequencies of metals was reported in 1949.

3 W. C. Dickinson, *Phys. Rev.* **1950**, *77*, 736.

4 W. G. Proctor, F. C. Yu, *Phys. Rev.* **1950**, *77*, 717.

5 H. S. Gutowsky, C. J. Hoffman, *Phys. Rev.* **1950**, *80*, 110.

6 I. Lindgren, *J. Electron Spectrosc. Relat. Phenom.* **2004**, *137–140*, 59. In the early 1920s, before the first observation of the chemical shift in ESCA, it was discovered that the wavelengths of X-ray radiation and the position of the absorption edge depend on the chemical environment of the atom.

7 K. Siegbahn, C. Nordling, A. Fahlman, R. Nordberg, K. Hamrin, J. Hedman, G. Johansson, T. Bergmark, S.-E. Karlsson, I. Lindgren, B. Lindberg, *ESCA Atomic, Molecular, and Solid State Structure Studied by Means of Electron Spectroscopy*, Almqvist & Wiksells Boktryckeri Ab, Uppsala, **1967**.

8 E. Sokolowski, C. Nordling, K. Siegbahn, *Phys. Rev.* **1958**, *110*, 776.

9 A. P. Hitchcock, D. C. Mancini, *J. Electron Spectrosc. Relat. Phenom.* **1994**, *67*, 1.

10 M. W. Dietrich, R. E. Keller, *Anal. Chem.* **1964**, *36*, 258.

11 T. A. Carlson, *Photoelectron and Auger Spectroscopy*, Plenum, New York, **1975**.

12 B. J. Lindberg, *J. Electron Spectrosc. Relat. Phenom.* **1974**, *5*, 149.

13 N. Inamoto, *Hammett Rule*, Maruzen, Tokyo, **1983**.

14 C. D. Johnson, *The Hammett Equation*, Cambridge University, London, **1973**.

15 W. J. Hehre, L. Radom, P. v. R. Schleyer, J. A. Pople, *Ab Initio Molecular Orbital Theory*, Wiley-Interscience, New York, **1986**.

16 T. J. Barton, A. Revis, I. M. T. Davidson, S. Ijadi-Maghsoodi, K. J. Hugles, M. S. Gordon, *J. Am. Chem. Soc.* **1986**, *108*, 4022.

17 S. Nagaoka, J. Ohshita, M. Ishikawa, T. Masuoka, I. Koyano, *J. Phys. Chem.* **1993**, *97*, 1488.

18 S. Nagaoka, J. Ohshita, M. Ishikawa, K. Takano, U. Nagashima, T. Takeuchi, I. Koyano, *J. Chem. Phys.* **1995**, *102*, 6078.

19 S. Nagaoka, K. Mase, M. Nagasono, S. Tanaka, T. Urisu, J. Ohshita, *J. Chem. Phys.* **1997**, *107*, 10751.

20 S. Nagaoka, T. Fujibuchi, J. Ohshita, U. Nagashima, I. Koyano, *Chem. Phys.* **2002**, *276*, 243.

21 H. Ohashi, E. Ishiguro, Y. Tamenori, H. Okumura, A. Hiraya, H. Yoshida, Y. Senba, K. Okada, N. Saito, I. H. Suzuki, K. Ueda, T. Ibuki, S. Nagaoka, I. Koyano, T. Ishikawa, *Nucl. Instrum. Methods Phys. Res., Sect. A* **2001**, *467–468*, 533.

22 K. Ueda, H. Yoshida, Y. Senba, K. Okada, Y. Shimizu, H. Chiba, H. Ohashi, Y. Tamenori, H. Okumura, N. Saito, S. Nagaoka, A. Hiraya, E. Ishiguro, T. Ibuki, I. H. Suzuki, I. Koyano, *Nucl. Instrum. Methods Phys. Res., Sect. A* **2001**, *467–468*, 1502.

23 S. Nagaoka, T. Ibuki, N. Saito, Y. Shimizu, Y. Senba, K.

Kamimori, Y. Tamenori, H. Ohashi, I. H. Suzuki, *J. Phys. B: At. Mol. Opt. Phys.* **2000**, *33*, L605.

24 S. Nagaoka, Y. Tamenori, M. Hino, T. Kakiuchi, J. Ohshita, K. Okada, T. Ibuki, I. H. Suzuki, *Chem. Phys. Lett.* **2005**, *412*, 459.

25 K. Siegbahn, N. Kholine, G. Golikov, *Nucl. Instrum. Methods Phys. Res., Sect. A* **1997**, *384*, 563.

26 K. Isari, E. Kobayashi, K. Mase, K. Tanaka, *Surf. Sci.* **2003**, *528*, 261.

27 K. Isari, H. Yoshida, T. Gejo, E. Kobayashi, K. Mase, S. Nagaoka, K. Tanaka, *J. Vac. Soc. Jpn.* **2003**, *46*, 377.

28 K. Mase, M. Nagasono, S. Tanaka, T. Sekitani, S. Nagaoka, *Fiz. Nizk. Temp.* **2003**, *29*, 321; K. Mase, M. Nagasono, S. Tanaka, T. Sekitani, S. Nagaoka, *Low Temp. Phys.* **2003**, *29*, 243.

29 S. Nagaoka, K. Mase, M. Nagasono, S. Tanaka, T. Urisu, J. Ohshita, U. Nagashima, *Chem. Phys.* **1999**, *249*, 15.

30 K. Mase, E. Kobayashi, A. Nambu, T. Kakiuchi, O. Takahashi, K. Tabayashi, M. Mitani, J. Ohshita, S. Nagaoka, unpublished work.

31 M. J. Frisch, G. W. Trucks, H. B. Schlegel, G. E. Scuseria, M. A. Robb, J. R. Cheeseman, V. G. Zakrzewski, J. A. Montgomery, Jr., R. E. Stratmann, J. C. Burant, S. Dapprich, J. M. Millam, A. D. Daniels, K. N. Kudin, M. C. Strain, O. Farkas, J. Tomasi, V. Barone, M. Cossi, R. Cammi, B. Mennucci, C. Pomelli, C. Adamo, S. Clifford, J. Ochterski, G. A. Petersson, P. Y. Ayala, Q. Cui, K. Morokuma, N. Rega, P. Salvador, J. J. Dannenberg, D. K. Malick, A. D. Rabuck, K. Raghavachari, J. B. Foresman, J. Cioslowski, J. V. Ortiz, A. G. Baboul, B. B. Stefanov, G. Liu, A. Liashenko, P. Piskorz, I. Komaromi, R. Gomperts, R. L. Martin, D. J. Fox, T. Keith, M. A. Al-Laham, C. Y. Peng, A. Nanayakkara, M. Challacombe, P. M. W. Gill, B. Johnson, W. Chen, M. W. Wong, J. L. Andres, C. Gonzalez, M. Head-Gordon, E. S. Replogle, J. A. Pople, *Gaussian 98, Revision A.11.3*, Gaussian, Pittsburgh, **2002**.

32 M. Takahashi, K. Sakamoto, M. Kira, *Int. J. Quantum Chem.* **2001**, *84*, 198.

33 T. Veszprémi, M. Takahashi, J. Ogasawara, K. Sakamoto, M. Kira, *J. Am. Chem. Soc.* **1998**, *120*, 2408.

34 J. R. Cheeseman, G. W. Trucks, T. A. Keith, M. J. Frisch, *J. Chem. Phys.* **1996**, *104*, 5497.

35 J. B. Foresman, Æ. Frisch, *Exploring Chemistry with Electronic Structure Methods*, 2nd ed., Gaussian, Pittsburgh, **1996**.

36 Æ. Frisch, M. J. Frisch, *Gaussian 98 User's Reference*, 2nd ed., Gaussian, Pittsburgh, **1999**, p. 43.

37 M. J. Frisch, G. W. Trucks, H. B. Schlegel, G. E. Scuseria, M. A. Robb, J. R. Cheeseman, J. A. Montgomery, Jr., T. Vreven, K. N. Kudin, J. C. Burant, J. M. Millam, S. S. Iyengar, J. Tomasi, V. Barone, B. Mennucci, M. Cossi, G. Scalmani, N. Rega, G. A. Petersson, H. Nakatsuji, M. Hada, M. Ehara, K. Toyota, R. Fukuda, J. Hasegawa, M. Ishida, T. Nakajima, Y. Honda, O. Kitao, H. Nakai, M. Klene, X. Li, J. E. Knox, H. P. Hratchian, J. B. Cross, C. Adamo, J. Jaramillo, R. Gomperts, R. E. Stratmann, O. Yazyev, A. J. Austin, R. Cammi, C. Pomelli, J. W. Ochterski, P. Y. Ayala, K. Morokuma, G. A. Voth, P. Salvador, J. J. Dannenberg, V. G. Zakrzewski, S. Dapprich, A. D. Daniels, M. C. Strain, O. Farkas, D. K. Malick, A. D. Rabuck, K. Raghavachari, J. B. Foresman, J. V. Ortiz, Q. Cui, A. G. Baboul, S. Clifford, J. Cioslowski, B. B. Stefanov, G. Liu, A. Liashenko, P. Piskorz, I. Komaromi, R. L. Martin, D. J. Fox, T. Keith, M. A. Al-Laham, C. Y. Peng, A. Nanayakkara, M. Challacombe, P. M. W. Gill, B. Johnson, W. Chen, M. W. Wong, C. Gonzalez, J. A. Pople, *Gaussian 03, Revision C.02*, Gaussian, Wallingford CT, **2004**.

38 E. D. Glendening, A. E. Reed, J. E. Carpenter, F. Weinhold, *NBO, Version 3.1*.

39 Æ. Frisch, M. J. Frisch, G. W. Trucks, *Gaussian 03 User's Reference*, Gaussian, Wallingford CT, **2003**, pp. 183–184.

40 K. Siegbahn, C. Nordling, G. Johansson, J. Hedman, P. F. Hedén, K. Hamrin, U. Gelius, T. Bergmark, L. O. Werme, R. Manne, Y. Baer, *ESCA Applied to Free Molecules*, North-Holland, Amsterdam, **1969**, pp. 104–109.

41 S. Hüfner, *Photoelectron Spectroscopy, Principles, and Applications*, 3rd ed., Springer-Verlag, Berlin, **2003**, pp. 61–69.

42 S. Huzinaga, J. Andzelm, M. Klobukowski, E. Radzio-Andzelm, Y. Sakai, H. Tatewaki, *Gaussian Basis Sets for Molecular Calculations*, Elsevier, Amsterdam, **1984**.

43 T. H. Dunning, Jr., P. J. Hay, *Modern Theoretical Chemistry*, ed. by H. F. Schaefer, III, Plenum, New York, **1977**, Vol. 3.

44 I. N. Levin, *Quantum Chemistry*, 5th ed., Prentice Hall, Upper Saddle River, **2000**, Section 15.4.

45 J. A. Pople, D. L. Beveridge, *Approximate Molecular Orbital Theory*, McGraw-Hill, New York, **1970**, Section 1.9 and Appendixes A and B.

46 J. D. Bozek, G. M. Bancroft, K. H. Tan, *Chem. Phys.* **1990**, *145*, 131.

47 J. D. Bozek, K. H. Tan, G. M. Bancroft, K. J. Fu, *Chem. Phys.* **1991**, *158*, 171.

48 S. Nagaoka, T. Fujibuchi, J. Ohshita, M. Ishikawa, I. Koyano, *Int. J. Mass Spectrom. Ion Processes* **1997**, *171*, 95.

49 C. F. Fischer, *The Hartree–Fock Method for Atoms—A Numerical Approach*, Wiley, New York, **1977**, p. 32.

50 K. Takano, H. Hosoya, S. Iwata, *J. Am. Chem. Soc.* **1984**, *106*, 2787.

51 P. Atkins, J. de Paula, *Atkins' Physical Chemistry*, 7th ed., Oxford University, Oxford, **2002**, Chap. 18.

52 F. Prosser, L. Goodman, *J. Chem. Phys.* **1963**, *38*, 374.

53 A. Gilbert, J. Baggott, *Essentials of Molecular Photochemistry*, Blackwell, Oxford, **1991**, pp. 87–89.

54 *Landolt–Börnstein, Numerical Data and Functional Relationships in Science and Technology, New Series, Group II: Atomic and Molecular Physics*, ed. by K.-H. Hellwege, A. M. Hellwege, Springer-Verlag, Berlin, **1976**, Vol. 7.

55 H. Sano, M. Katada, *Mössbauer Spectroscopy*, Gakkai Syuppan Center, Tokyo, **1996**, Chap. 2.

56 O. C. Kistner, A. W. Sunyar, *Phys. Rev. Lett.* **1960**, *4*, 412.

57 R. L. Mössbauer, *Nobel Lectures, Physics 1942–1962*, Elsevier, Amsterdam, **1964**, pp. 584–601.

58 R. H. Herber, *Inorg. Chim. Acta* **1974**, *8*, 10.

59 D. W. Ball, *Spectroscopy* **2003**, *18*, 70.

60 E. W. Weisstein, *Eric Weisstein's World of Physics*, Wolfram Research, Champaign, **2003**, http://scienceworld.wolfram.com/physics/MoessbauerSpectroscopy.html (accessed February 2006).

61 L. R. Walker, G. K. Wertheim, V. Jaccarino, *Phys. Rev. Lett.* **1961**, *6*, 98.

62 *DOE Fundamentals Handbook, Nuclear Physics and Reactor Theory*, U.S. Department of Energy, Washington, D.C., **1993**, Vol. 1 of 2, Module 1, pp. 6–7, http://www.eh.doe.gov/techstds/standard/hdbk1019/h1019v1.pdf (accessed February 2006).